Supplementary Information

Towards long-term stable $MAPbBr_3$ single crystal-based photoconductor with a high on/off ratio and detectivity

Vishnu Anilkumar,[a] Apurba Mahapatra,[a,*] Joanna Kruszyńska,[a] Manoranjan Mandal,[b] Seckin Akin,[c] Pankaj Yadav[d] and Daniel Prochowicz[a,*]

[a] Institute of Physical Chemistry, Polish Academy of Sciences, Kasprzaka 44/52, 01-224 Warsaw, Poland

[b] Department of Physics, School of Science, GITAM University, Bengaluru, 561203, India

[c] Department of Metallurgical and Materials Engineering, Necmettin Erbakan University, Konya, 42090, Turkey

[d] Department of Solar Energy, School of Energy Technology, Pandit Deendayal Energy University, Gandhinagar-382 007, Gujarat, India

1. Experimental Section

1.1 Materials

Lead (II) bromide ($PbBr_2$, ≥98%), toluene (Anhydrous, 99.8 %), isopropyl alcohol (IPA, 99.9%), dimethyl formamide (DMF, anhydrous 99.8%), octylamine (≥99 %) and Sulphuric acid were obtained from Sigma-Aldrich, methylammonium bromide (MABr, >99.99%) was obtained from Great Cell Solar Materials. All chemicals were used as received without any further purification.

1.2 Growth and Characterization of $MAPbBr_3$ SC: 1.2 M $MAPbBr_3$ solution was prepared by dissolving the equimolar amounts of $PbBr_2$ and MABr in 5 mL anhydrous DMF and stirring the solution at room temperature until a clear solution was obtained. The resulting clear solution was then filtered using a 0.2 µm PTFE filter. Subsequently, the solution was heated to 80°C and maintained at this temperature until large single crystals of $MAPbBr_3$ were formed. The resulting crystals were then collected, dried, and stored for further experiments.

1.3 Passivation process and characterization: A 4 mM sulfate passivation solution is prepared by dissolving an equimolar amount of octylamine and sulfuric acid in an IPA:toluene (1:5) mixture. The solution is stirred for 30 minutes and left undisturbed for 24 hours to stabilise. Afterwards, the solution is filtered using a PTFE 0.2 µm filter and then used for passivation. For the passivation process, the $MAPbBr_3$ SCs are fully immersed in the solution for 10, 20, 30, and 40 seconds, respectively. The SCs retrieved from the solution are washed with toluene, dried, and stored.

1.4 Fabrication and Characterizations of SC-based PDs: 100 nm thick platinum (Pt) electrodes were deposited on the (100) facet of SCs with a self-designed mask of 150 µm channel by using magnetron sputtering (Leica EM MED020). All current-voltage and PD response measurements were conducted using a Bio-Logic SP-150e potentiostat and a Semiconductor Analysis and Testing Solutions (SATs) probe station at a scan rate of 100 mV s^{-1}. The power of the blue LED (λ= 448 nm, Luxeon Star LED) was optimised using Thorlabs GmbH., PM 100D and controlled by Bio-Logic SP-150e potentiostat.

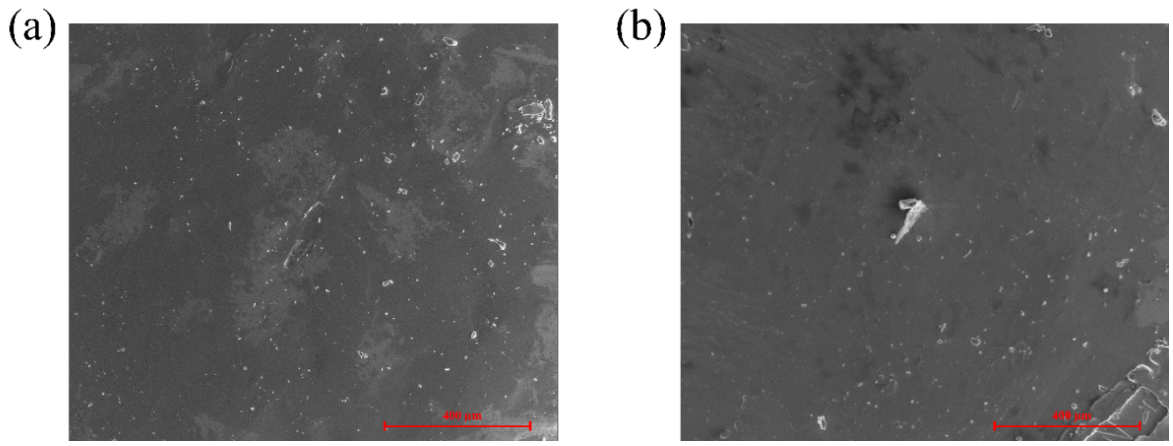

Fig. S1 SEM images of $MAPbBr_3$ SC surface (a) before and (b) after passivation.

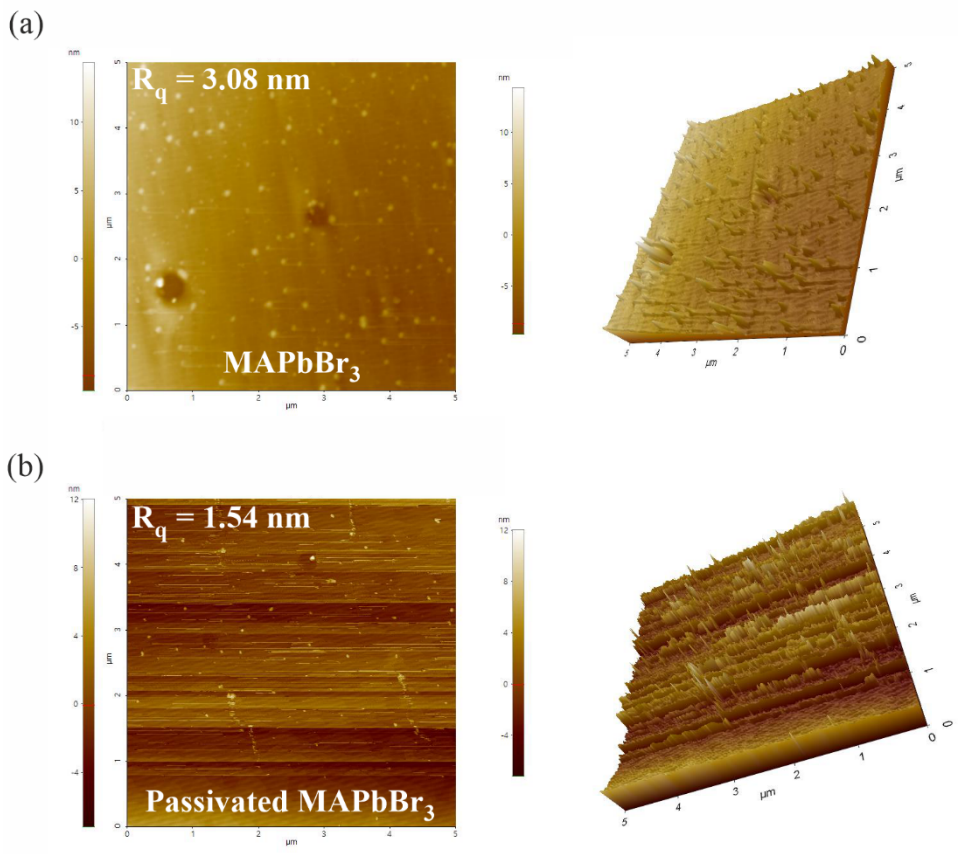

Fig. S2 AFM images of $MAPbBr_3$ SC surface (a) before and (b) after passivation.

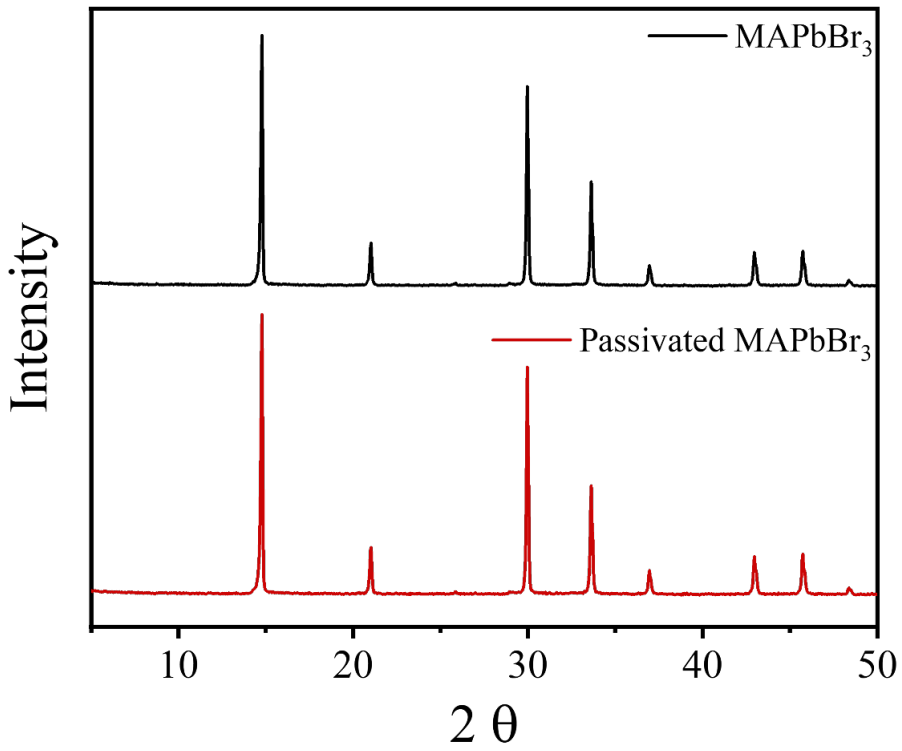

Fig. S3 The pXRD pattern of the pristine and passivated $MAPbBr_3$.

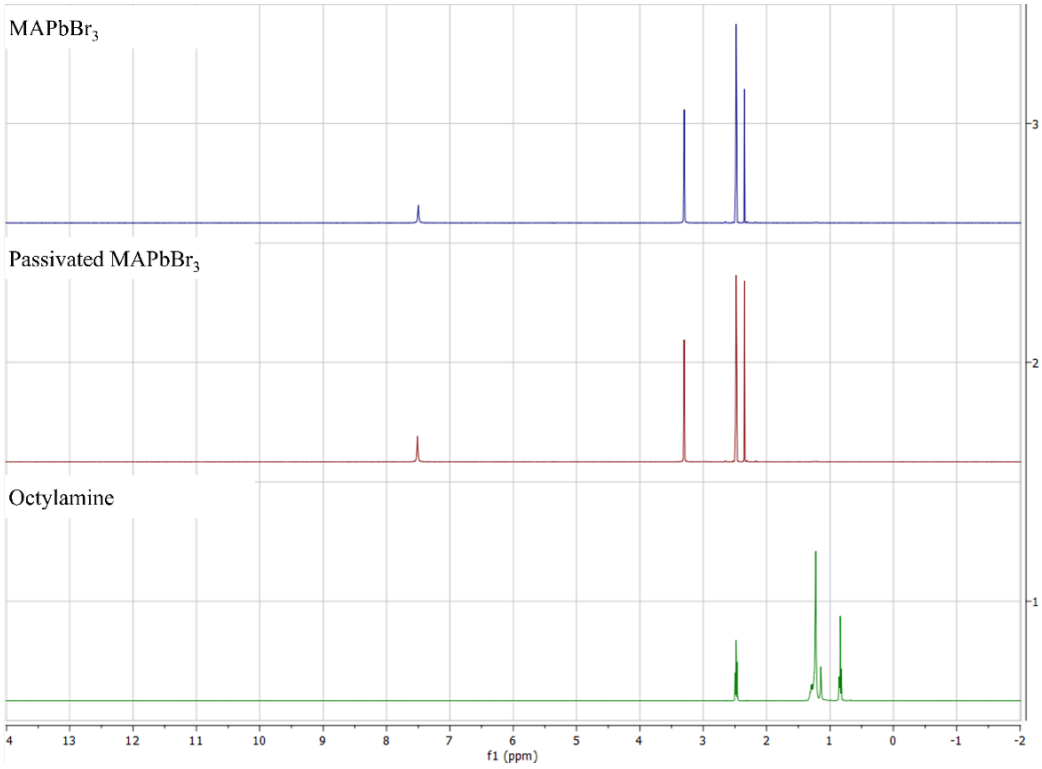

Fig. S4 ^1H NMR of the $MAPbBr_3$, passivated $MAPbBr_3$ and octylamine.

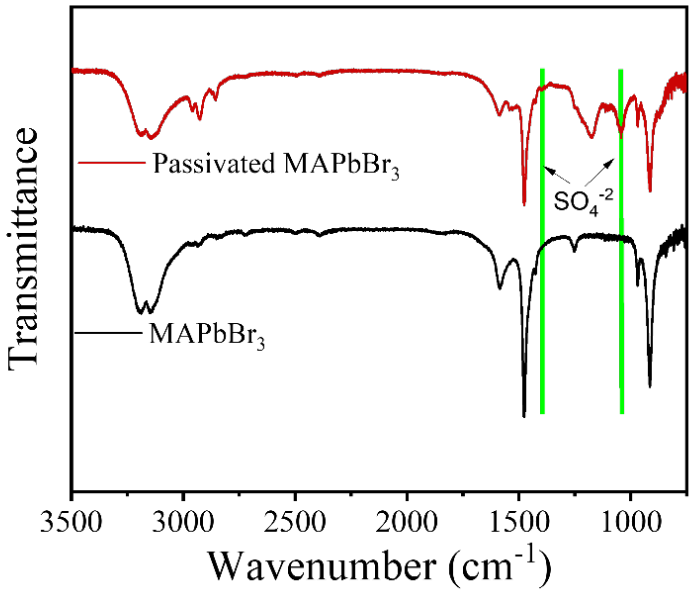

Fig. S5 FT-IR spectra of pristine $MAPbBr_3$ and passivated $MAPbBr_3$ SCs. The formation of $PbSO_4$ on the surface was confirmed by Fourier transform infrared (FT-IR) transmission measurement, which is consistent with our previous work.[1] The FTIR of the passivated SC confirms the presence of the character peaks of SO_4^{2-} (S=O stretching) at 1040 cm^{-1} and 1398 cm^{-1}. [1]

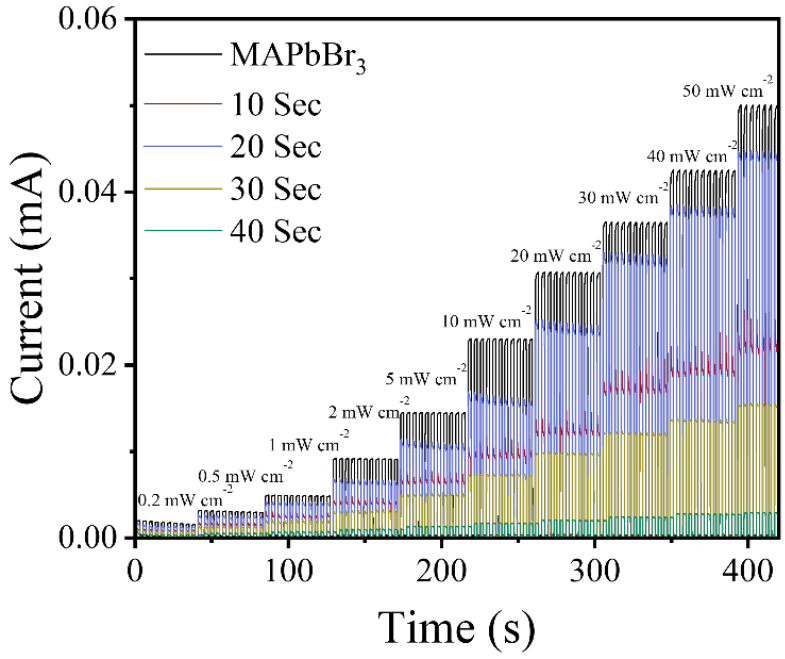

Fig. S6 Intensity-dependent transient photoresponse of the pristine, and 10, 20, 30, 40 seconds passivated $MAPbBr_3$ SC-based PDs under blue LED (λ = 448 nm) pulsed light at a fixed bias of 2 V.

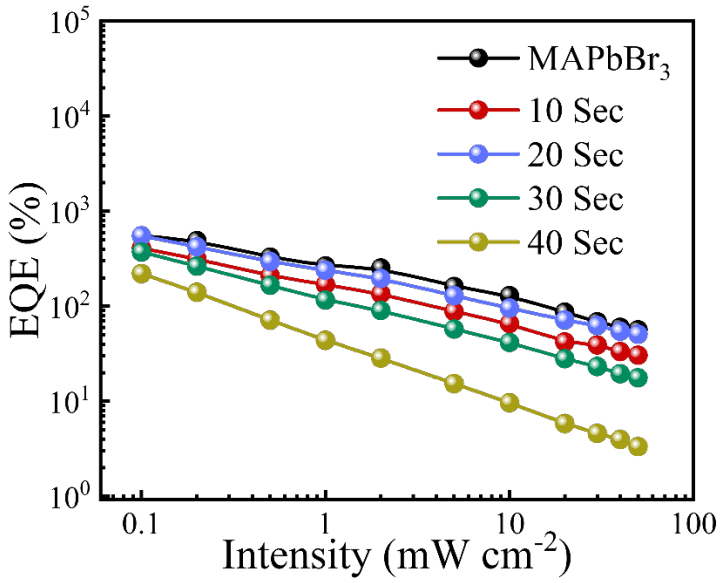

Fig. S7 EQE of the control and passivated SC-based PDs under blue light (448 nm) and 2 V bias.

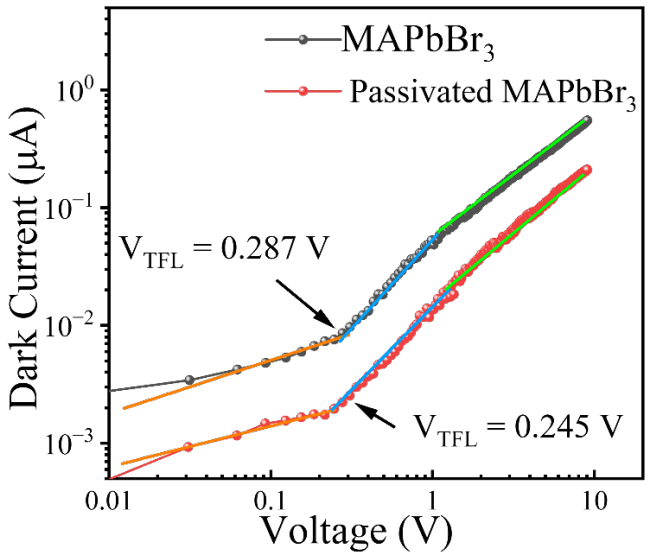

Fig. S8 Dark I–V characteristics in the form of SCLC of the pristine and passivated $MAPbBr_3$ SC.

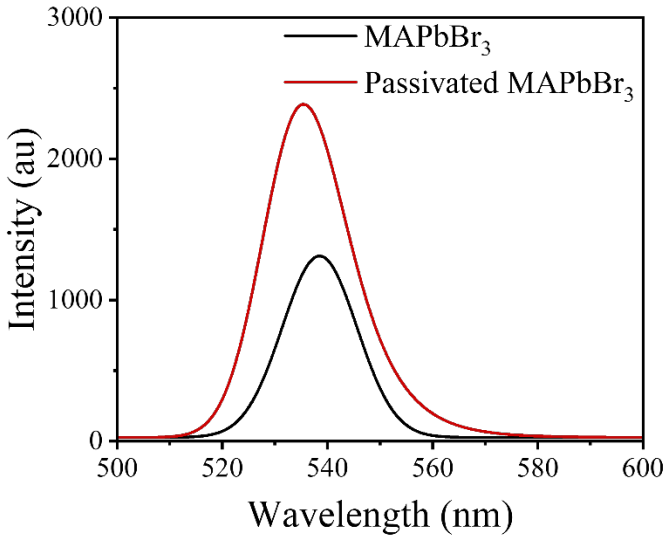

Fig. S9 The PL of the pristine and passivated SC for the excitation of 405 nm wavelength.

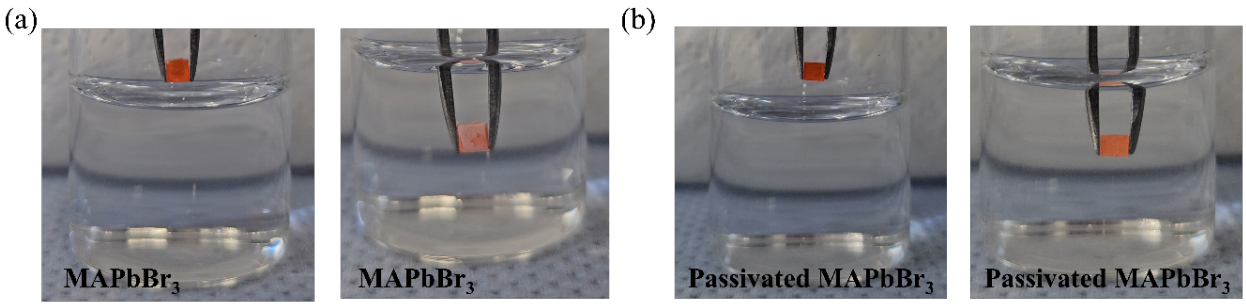

Fig. S10 (a) Pristine and (b) passivated $MAPbBr_3$ SCs immersed in water for 3 seconds.

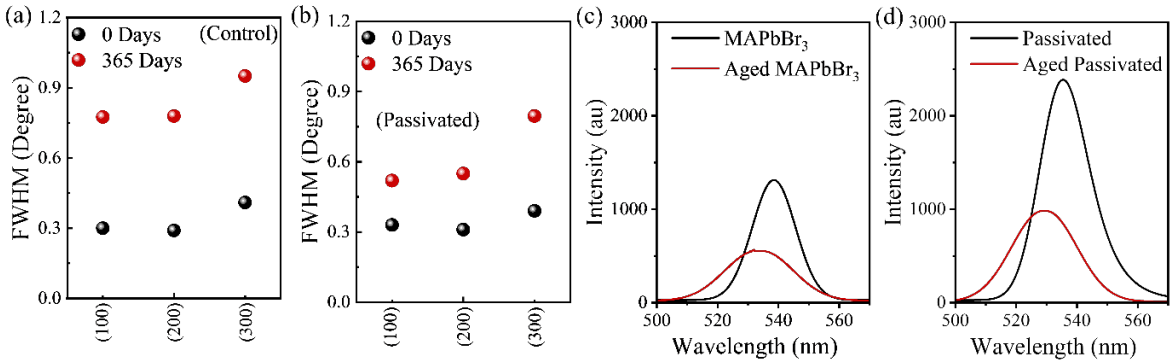

Fig. S11 Analysis of FWHM for the XRD peaks of fresh and aged (a) Pristine and (b) passivated $MAPbBr_3$ SCs. The evolution of PL spectra of (a) Pristine and (b) passivated $MAPbBr_3$ SCs over time.

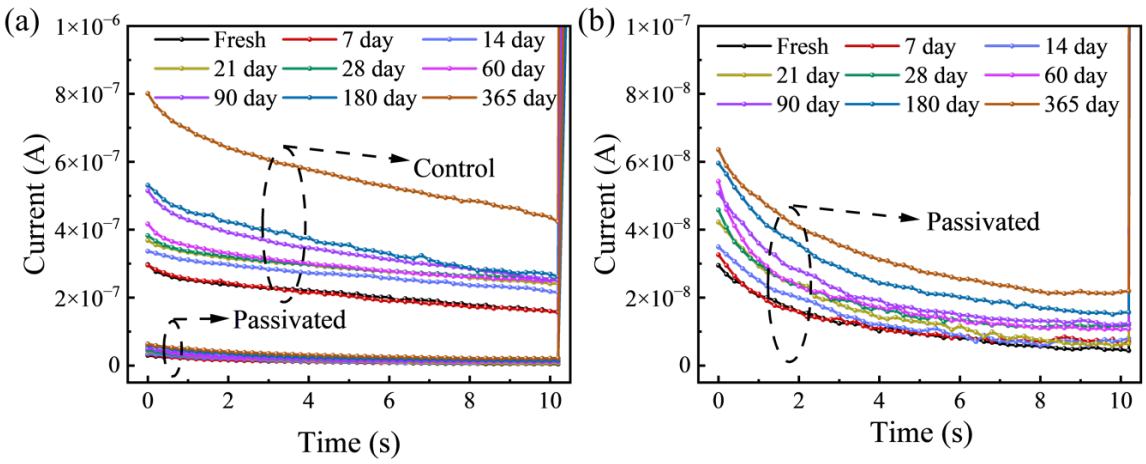

Fig. S12 Dark current of the (a) control and (b) 20 s dipped $MAPbBr_3$ SC-based PDs over aging time.

Supplementary Note 1

The responsivity (R) and external quantum efficiency (EQE) of the control and passivated SC-based PDs were calculated using Eqn. (S1) and (S2),[2]

$$Responsivity\ (R) = \frac{I_{light} - I_{dark}}{P \times A} \quad \text{---------- (Eqn. S1)}$$

Where I_{light} is photocurrent, I_{dark} is dark current, P is the illumination power, and A is the active area.

$$External\ quantum\ efficiency\ (EQE) = \frac{R \times h \times c}{\lambda \times e} \quad \text{---------- (Eqn. S2)}$$

where h is the plank's constant, λ is the illumination wavelength, and e is the elemental charge of the electron.

The responsivity Specific detectivity (D*) and on-off ratio of PDs are calculated as,[2]

$$Specific\ detectivity\ (D^*) = R\sqrt{\frac{A}{2 \times e \times I_{dark}}} \quad \text{---------- (Eqn. S3)}$$

$$on - off\ ratio = \frac{I_{light}}{I_{dark}} \quad \text{---------- (Eqn. S4)}$$

The trap density (η_{trap}) of these SCs was calculated using the space charge-limited current (SCLC) method as,[3]

$$\eta_{traps} = \frac{2\varepsilon_0 \varepsilon_r V_{TFL}}{eL^2} \quad \text{---------- (Eqn. S5)}$$

where ε_0 and ε_r are the dielectric constants of the vacuum permeability and the dielectric constant, and L is the thickness of the crystal.

The dark current (J_d) increasing rate is calculated using Eqn. (S6)[4]

$$Rate = \left(\frac{(J_a - J_b)/(a-b)}{J_b}\right) \times 100\% \quad \text{---------- (Eqn. S6)}$$

Where, the J_a and J_b are the dark current densities of the days a and b.

Table S1. The comparison of PD parameters for $MAPbBr_3$ SC-based photoconductor with symmetric electrode reported in the literature and our work.

PD structure	Wavelength (nm)	Light Intensity	Bias (V)	Distance between electrodes	R (A/W)	EQE (%) / Gains	D (Jones)	Ref
Au/ $MAPbBr_3$/Au	405	10 µW	9.84	100 µm	0.015 (100)	0.046		**5**
					0.038 (110)	0.113		
Au/ $MAPbBr_3$/Au	576	1 W m^{-2}	2	125 µm	0.6	124	4×10^{11}	**6**
				100 µm	0.7	151	2.5×10^{11}	
				75 µm	1.02	221	2.5×10^{11}	
				50 µm	1.31	298	2.2×10^{11}	
				25 µm	1.54	332	2.2×10^{11}	
		0.02 W m^{-2}		125 µm	2.3	498	1.4×10^{12}	
				100 µm	2.8	607	1×10^{12}	
				75 µm	3.3	705	8×10^{11}	
				50 µm	4.2	900	7.2×10^{11}	
				25 µm	5.3	1130	7.4×10^{11}	
Au/Cr/ $MAPbBr_3$/ Cr/Au	525	0.012 mW cm^{-2}	4		16	3900	6×10^{13}	**7**
Au/ $MAPbBr_3$ (concave)/Au	520	3.67 µW cm^{-2}	3		62.9	1.50×10^4	6.5×10^{12}	**8**
		12.02 µW cm^{-2}			58.5	1.4×10^4		
		35.4 mW cm^{-2}			5.43	1300	6.5×10^{12}	
Au/$MAPbBr_3$ /Au	520	35.4 mW cm^{-2}	3		0.98	234	6.5×10^{12}	
Au/$MAPbBr_3$ /Au	630	0.1 mW	5		1.7×10^{-3}	0.22		**9**

Au/Cr/ $MAPbBr_3$/ Cr /Au	515	10^{-3} mW cm^{-2}	5		55.7	13453	8×10^{13}	**10**
		35 mW cm^{-2}			≈ 0.1	≈ 40	≈ 2.5 6.5 × 10^{11}	
		0.1 mW cm^{-2}			≈ 3	≈ 8×10^3	≈ 5×10^{12}	
Au/ $MAPbBr_3$ /Au	448	0.1 mW cm^{-2}	2	150 µm	0.41	112	1.05 × 10^{12}	**11**
Pt/ $MAPbBr_3$ /Pt					1.99	553	5.09 × 10^{12}	
Pt/ passivated-$MAPbBr_3$ /Pt	**448**	**0.1 mW cm^{-2}**	**2**	**150 µm**	**1.99**	**552**	**1.7×10^{13}**	**This work**
Pt/ $MAPbBr_3$ /Pt					**1.99**	**552**	**4.9×10^{12}**	

References

1 A. Mahapatra, N. Parikh, H. Kumari, M. K. Pandey, M. Kumar, D. Prochowicz, A. Kalam, M. M. Tavakoli and P. Yadav, *J. Appl. Phys.*, 2020, **127**, 185501.

2 V. Anilkumar, A. Mahapatra, J. Nawrocki, R. D. Chavan, P. Yadav and D. Prochowicz, *Adv. Optical Mater.*, 2024, **12**, 2302032.

3 A. Mahapatra, V. Anilkumar, J. Kruszyńska, N. Mrkyvkova, P. Siffalovic, P. Yadav and D. Prochowicz, *J. Mater. Chem. C*, 2024, **12**, 2953–2960.

4 Y. Xu, X. Wang, J. Zhao, Y. Pan, Y. Li, E. E. Elemike, Q. Li, X. Zhang, J. Chen, Z. Zhao, J. Akram, B. S. Bae, S. Bin and W. Lei, *Front. Mater.*, 2021, **8**, 651957

5 Z. Zuo, J. Ding, Y. Zhao, S. Du, Y. Li, X. Zhan and H. Cui, *J. Phys. Chem. Lett.*, 2017, **8**, 684–689.

6 S. Gavranovic, J. Pospisil, O. Zmeskal, V. Novak, P. Vanysek, K. Castkova, J. Cihlar and M. Weiter, *ACS Appl. Mater. Interfaces*, 2022, **14**, 20159–20167.

7 Y. Liu, Y. Zhang, K. Zhao, Z. Yang, J. Feng, X. Zhang, K. Wang, L. Meng, H. Ye, M. Liu and S. (Frank) Liu, *Adv. Mater.*, 2018, **30**, 1707314.

8 H. Liu, X. Wei, Z. Zhang, X. Lei, W. Xu, L. Luo, H. Zeng, R. Lu and J. Liu, *J. Phys. Chem. Lett.*, 2019, **10**, 786–792.

9 Z. Zhang, K. Chen, W. Xia and Z. Zuo, *Mater. Res. Express*, 2020, **7**, 125902.

10 Y. Liu, Y. Zhang, Z. Yang, J. Feng, Z. Xu, Q. Li, M. Hu, H. Ye, X. Zhang, M. Liu, K. Zhao, S. (Frank) Liu *Mater. Today*, 2019, **22**, 67–75.

11 A. Mahapatra, V. Anilkumar, R. D. Chavan, P. Yadav and D. Prochowicz, *ACS Photonics*, 2023, **10**, 1424–1433.